THE ARCHIVES OF MECHANICAL ENGINEERING

VOL. LIII 2006 Number 4

Key words: turbine engine, transient processes, mathematical modelling, digital simulation

WOJCIECH I. PAWLAK *

THE EFFECT OF CONVERGENT-NOZZLE VOLUME ON TRANSIENT PROCESSES IN A TURBOJET ENGINE

The effect of processes of accumulating mass and enthalpy of the working medium on the dynamics of transient processes thereof is often discussed in scientific publications on the mathematical modelling of turbine engines (treated as systems that undergo control and automatic adjustment). The paper is intended to make a comparison between findings gained from simulation carried out with two alternative models of an aircraft turbine engine (of the SO-3 type). The first model takes account of the dynamics of the processes of accumulating mass and energy of the working medium within the combustion-chamber volume and that of the convergent nozzle. The second, simplified model, neglects the dynamics of the processes of accumulating mass and energy of the working medium, since it has been assumed that it is the dynamics of the kinetic-energy accumulation in the rotor mass that predominates in various representations of transient processes. To conduct simulation-based experiments, each of the alternative models of an engine was connected to a special simulation unit, which simulated operation of fuel supply and control systems. Two rounds of experiments were carried out. The first one was intended to facilitate observations of transient processes effected with quick shifting of a control lever from the idle position to that of full thrust, and back. In the second round observed were processes resulting from changes in the critical jet area. The second, alternative model was used to investigate the effect of ever-greater hypothetical volumes of the nozzle on how the transient processes proceeded. It has been found that in the case of the SO-3 engine, low nozzle capacity remains of only slight effect on how the transient processes proceed. Hence, simplified modelling methodology is fully justified.

* *Air Force Institute of Technology; Księcia Bolesława Str. 6, 01-494 Warsaw 46 PB. 96; E-mail: pawlakizydor.wojciech@acn.waw.pl*

Graphic symbols

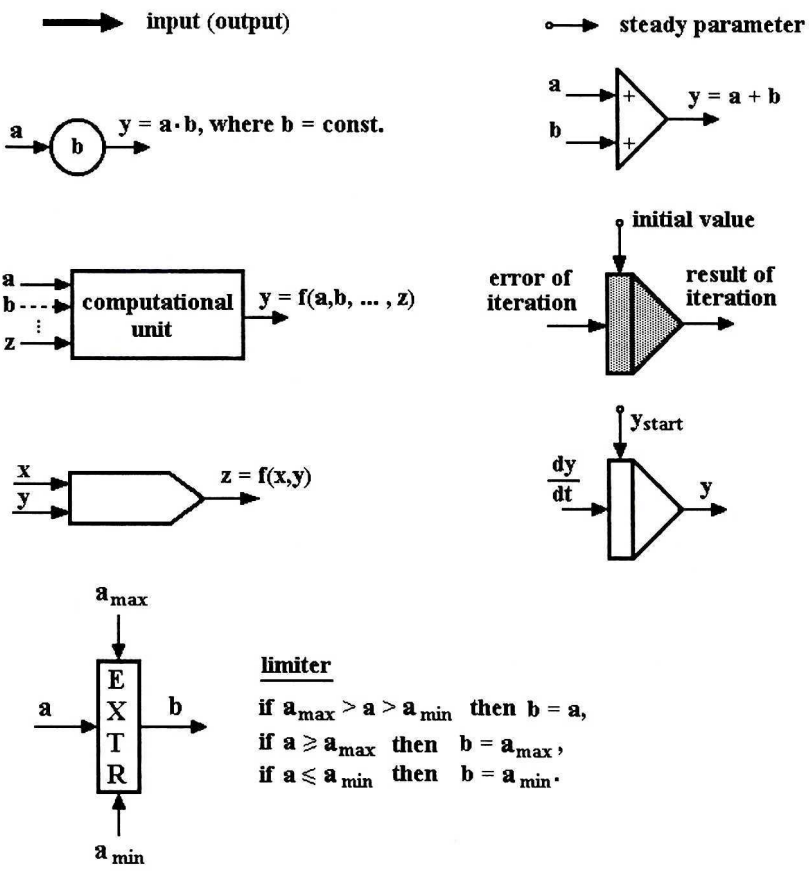

Nomenclature

A_d – conventional accumulation space of the convergent nozzle (simulation model's unit),

A_{ks} – conventional accumulation space of the convergent nozzle (simulation model's unit),

Cp_{12} – average specific heat of the working medium in the compressor duct,

Cp_{23} – average specific heat of the working medium in the combustion chamber,

Cp_{34} – average specific heat of the working medium in the turbine duct,

Cp_{45} – average specific heat of the working medium in the convergent nozzle,

D – convergent nozzle,

Delta_n – control error of the maximum-rotational-speed limiter,
fkr – critical jet area of the convergent nozzle,
G2 – mass flow of the working medium at the compressor outlet,
$G2_r$ – reduced mass flow of the working medium at the compressor outlet,
G3 – mass flow of the working medium at the combustion chamber outlet,
G3t – reduced mass flow of the working medium through the turbine,
Ga – mass flow of the working medium at the entry into the 'V' volume,
Gb – mass flow of the working medium at the exit out of the 'V' volume,
I – enthalpy of the working medium accumulated in the 'V' volume,
I_d – enthalpy of the working medium accumulated in the convergent nozzle,
I_{ks} – enthalpy of the working medium accumulated in the combustion chamber,
I_o – polar moment of inertia of the rotor of the turbine-compressor assembly,
k – exponent of isentrope of the working medium accumulated in the 'V' volume,
k_{23} – average exponent of isentrope of the working medium in the combustion chamber,
k_{34} – average exponent of isentrope of the working medium in the turbine duct,
k_{45} – average exponent of isentrope of the working medium in the convergent nozzle,
KS – combustion chamber,
LSU – steady-state line,
M – Mach number (here: air speed),
m – mass of the working medium accumulated in the 'V' volume,
m_d – mass of the working medium accumulated in the convergent nozzle,
m_{ks} – mass of the working medium accumulated in the combustion chamber,
n – rotational speed of the rotor,
N_s – input power of the compressor,
N_{sr} – reduced rotational speed of the compressor,
N_{start} – initial rotational speed of the rotor,
n – rotational speed of the rotor,
n_bj – idle run rotational speed of the rotor,

n_max – maximum-rotational-speed of the rotor,
N_t – turbine power,
N_{tr} – reduced rotational speed of the turbine,
P – average impact pressure of the working medium accumulated in the 'V' volume,
P0 – impact pressure of the working medium at the engine inlet,
P1 – impact pressure of the working medium in front of the compressor,
$P2_{start}$ – initial average impact pressure of the working medium behind the compressor,
P4 – impact pressure of the working medium in the convergent nozzle,
$P4_{start}$ – initial average impact pressure of the working medium in the convergent nozzle (in the Model B),
Pd_{start} – initial average impact pressure of the working medium in the volume A_d (in the Model A),
PH – ambient pressure,
Pks_{start} – initial average impact pressure of the working medium in the combustion chamber,
pQ – first derivative of the rate of fuel flow,
pQmax – upper limit of the first derivative of the rate of fuel flow in transient states,
pQmin – lower limit of the first derivative of the rate of fuel flow in transient states,
Q – rate of fuel flow,
Qmax – maximum rate of fuel flow,
Q_start – initial rate of fuel flow,
Qd – lower limit of the rate of fuel flow in transient states,
Qg – upper limit of the rate of fuel flow in transient states,
Rg – gas constant,
T – average impact temperature of the working medium accumulated in the 'V' volume,
T1 – impact temperature of the working medium in front of the compressor,
T2 – impact temperature of the working medium behind the compressor,
T3 – impact temperature of the working medium in front of the turbine,
T4 – impact temperature of the working medium behind the turbine,
T4t – temperature of the working medium measured with a set of thermocouples,

Ta – impact temperature of the working medium at the entry into the 'V' volume,
TauASS – time constant of the rate-of-flow control unit,
Tb – temperature of the working medium at the exit out of the 'V' volume,
Td_{start} – initial average impact temperature of the working medium in the convergent nozzle,
Tks_{start} – initial average impact temperature of the working medium in the combustion chamber,
U_1 – error of iteration,
U_2 – error of iteration,
V – volume of the selected part of the engine-duct space,
V_d – volume of the duct of convergent nozzle,
V_{ks} – volume of the combustion-chamber duct,
W_1 – factor of amplification of iterative loop,
W_2 – factor of amplification of iterative loop,
Wo – fuel calorific value,
Wu – air bleed coefficient,
WzmPR – coefficient of proportional amplification of the rotational-speed control unit (limiter),
WzmQ – amplification factor of the rate-of-fuel control unit,
α DSS – angle of the engine-control-lever setting,
Δ T12 – increment of temperature of the working medium due to compression,
Π – pressure ratio (of the compressor),
ε – pressure ratio of decompression of the working medium while flowing through the turbine,
ϕ – rate-of-flow coefficient of a convergent nozzle,
η_{ks} – efficiency of heat emission in the combustion chamber,
η_{ms} – coefficient of mechanical efficiency of combustion chamber,
η_{mt} – coefficient of mechanical efficiency of the turbine,
η_t – isentropic efficiency of the turbine,
ρ – average specific density of the working medium accumulated in the 'V' volume,
σ_{23} – the impact-pressure-retention coefficient for the combustion-chamber flow,
σ_{01} – the impact-pressure-retention coefficient for the compressor flow.

1. Introduction

In the available literature on the mathematical modelling of turbine engines treated as systems under control [1], [3], [4], [7], [8], [14], the question of whether account should (or should not) be taken of the dynamics of processes of accumulating mass and enthalpy of the working medium in some selected volumes of the engine duct remains a question that all the time gives rise to much controversy. Predominating are opinions on both the suitability and need to take these phenomena into consideration [1], [3], [4], [14]. In consequence, due to relatively high rates of the processes of mass accumulation and enthalpy, a suitable digital simulation model requires short-step (approx. 0.5ms) integration. This, however, significantly extends time needed for simulated processes. In the case no account is taken of the processes of accumulating mass and enthalpy of the working medium, the required integration step can be many times longer (approx. 0.02s). However, there is another problem related to the application of a suitably fast and stable algorithm of solving the system of non-linear algebraic equations with the iteration method (Fig. 6). On the other hand, the simulation model that takes account of the dynamics of the processes of accumulating mass and enthalpy of the working medium does not include the system of algebraic equations. It only includes an algorithm of numerical integration of the system of ordinary non-linear differential equations (Fig. 2). The model of an engine, which takes account of the dynamics of the processes of accumulating mass and enthalpy of the working medium, is further on called 'Model A', whereas the model with the dynamics of these processes neglected – 'Model B'.

To recapitulate, Model A has been applied to examine the effect of the nozzle volume on the dynamics of transient processes, whereas Model B – as that offering comparative basis to find an answer to the following question: To what extent is it reasonable to reduce the dynamics of transient processes in a turbine engine down to the dynamics of accumulating the kinetic energy in the rotor mass?

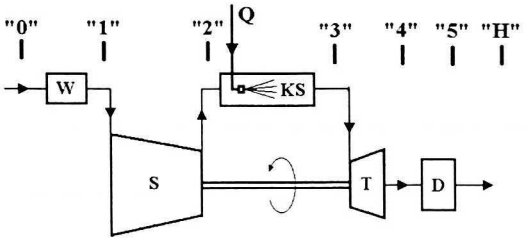

Fig. 1. Computational diagram of the SO-3 engine (W – inlet, S – compressor, KS – combustion chamber, T – turbine, D – convergent nozzle, Q – rate of fuel flow)

Fig. 1 presents a computational diagram of the SO-3 jet engine, with all the structural assemblies and assumed computational cross-sections of the duct – indicated. To keep descriptions of the models concise, most of the equations used to formulate these models have not been given here *explicite*, since they are to be found in the publications and handbooks on the thermodynamics, the fluid mechanics, and the theory of heat engines. Major attention has been paid to analogue and block diagrams intended to show – in some well-ordered way – the connections between all variables and parameters of the models. The enclosed Nomenclature list facilitates the studying of these diagrams.

2. Model A

A block diagram of the simulation model consists of two parts. The first one, shown in Fig. 2, refers to a system of non-linear differential equations that describe the working-medium flow in the engine duct. The second one, shown in Fig. 3, refers to a differential equation of motion of the rotor of the turbine-compressor assembly.

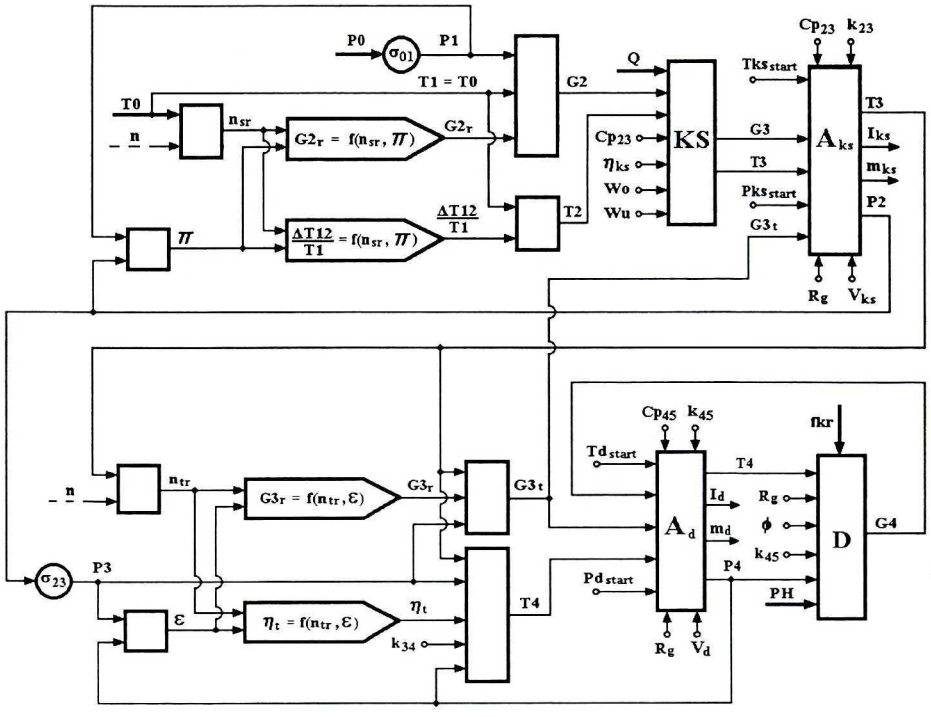

Fig. 2. Model A. A block diagram of the system of integrating differential equations that describe parameters of the working-medium flow

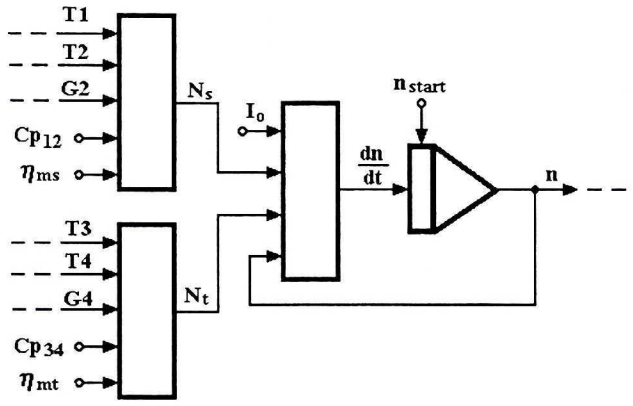

Fig. 3. Model A and Model B. A block diagram of the system of integrating equations of motion of the rotor

In the structure of the first part incorporated are blocks 'A_{ks}' and 'A_d', which comprise differential equations that describe processes of accumulating mass and enthalpy of the working medium within the volume of the combustion chamber (A_{ks}) and that of the convergent nozzle (A_d). Both two blocks show identical structures, presented in full detail in Fig. 4. They have been built on the grounds of a system of equations (1–6).

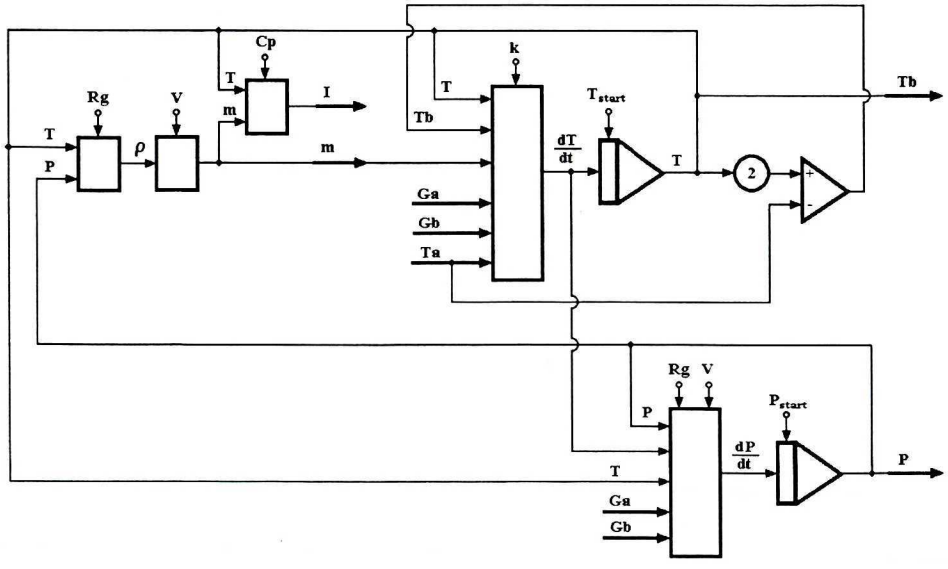

Fig. 4. Model A. A block diagram of the system of integrating equations of accumulation of mass and enthalpy of the working medium within the volume of the combustion chamber (V_{ks}) or the nozzle (V_d)

The additional figure, Fig. 5, shows the ordering of input and output variables and pre-set parameters of the A_{ks} and A_d blocks. In order to do that, notation admitted in the system of equations (1–6) has been applied.

$$Tb = 2 * T - Ta; \tag{1}$$

$$\rho = \frac{P}{Rg * T}; \tag{2}$$

$$m = V * \rho; \tag{3}$$

$$I = Cp * T * m; \tag{4}$$

$$\frac{dT}{dt} = \frac{1}{m}\left[Ga * (k * Ta - T) + Gb * (T - k * Tb)\right]; \tag{5}$$

$$\frac{dP}{dt} = (Ga - Gb) * \frac{Rg * T}{V} + \frac{P}{T} * \frac{dT}{dt}. \tag{6}$$

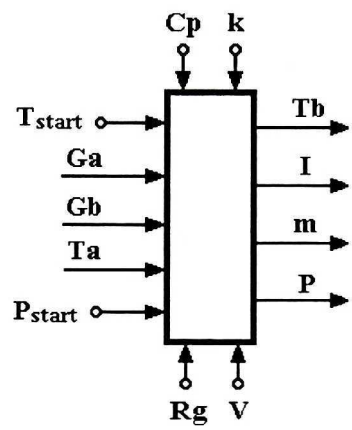

Fig. 5. The arrangement of input/output variables and constant parameters of the block diagram shown in Fig. 4

An alternative solution of the structure of the A_{ks} block can be found in the literature [1], [3], [4], [14]. It consists in matching equations (1–6) with the equation of heat balance of the combustion chamber. The equation of heat balance of the combustion chamber appears in the structure of the model shown in Fig. 2 in a separate block KS. It has been proved that both modelling techniques bring about exactly the same results.

The process of accumulating mass and enthalpy of the working medium has been assumed to proceed in two volumes only, i.e. the combustion chamber (A_{ks}) and the convergent nozzle (A_d). On the other hand, similar processes taking place in the inlet duct, in the compressor and the turbine have been neglected. The neglect of the inlet duct has been justified with that the planned simulation-based experiments are limited to running an engine with short inlet duct only. The neglect of little volume of the turbine duct results from the turbine being single-stage. The model does not separately show the volume of the compressor duct, since – for the need of experiments – this quantity has been assumed included in the combustion-chamber volume.

Model A is featured with what follows: in each subsequent integration step, for the known initial values of all integrating elements (n_{start}, Tks_{start}, Pks_{start}, Td_{start}, Pd_{start}) one can easily calculate values of all derivatives present in differential equations (dn/dt, dTks/dt, dPks/dt, dTd/dt, dPd/dt).

3. Model B

A block diagram of the model B also consists of two parts. The first one, shown in Fig. 6, refers to a system of non-linear algebraic equations that describe the working-medium flow in the engine duct. The second one, the same as for model A (Fig. 3), refers to a differential equation of motion of the rotor of the turbine-compressor assembly. It has been assumed that processes of accumulating enthalpy and mass of the working medium in some selected portions of the engine duct are so fast (as compared with the process of kinetic-energy accumulation in the rotor) that can be treated as quasi-static. Therefore, algebraic equations have been used to describe parameters of the working medium in the engine duct in transient states. Hence, in this case of a simulation model there is only one differential equation that describes the process of accumulating kinetic energy in the rotor (Fig. 3).

Model B is featured with what follows: in each subsequent step of integrating the rotor-motion equation, for some known initial values of rotational speed (n_{start}), there is no simple way to calculate the value of its derivative (dn/dt). One should, therefore, apply the method of iteration; this is clearly shown in Fig. 6. The suggested method is one of many others applicable in such a case. What is of significance resolves itself to a program code of the iteration algorithm operating quickly and in a stable way. Results of multiple tests have proved that the Euler method used exactly as shown in Fig. 3 is the best. Anyway, on the grounds of initial values ($P2_{start}$ and $P4_{start}$), a sequence of iterations is performed in each integration step, where subsequent iterated values (P2 and P4) are calculated in the following way:

$$P2 = P2_{\text{start}} + u_1 * w_1; \tag{7}$$

$$P4 = P4_{\text{start}} + u_2 * w_2; \tag{8}$$

In each subsequent iteration step new initial values are assumed – by means of substitution:

$$P2_{\text{start}} = P_2; \tag{9}$$

$$P4_{\text{start}} = P_4; \tag{10}$$

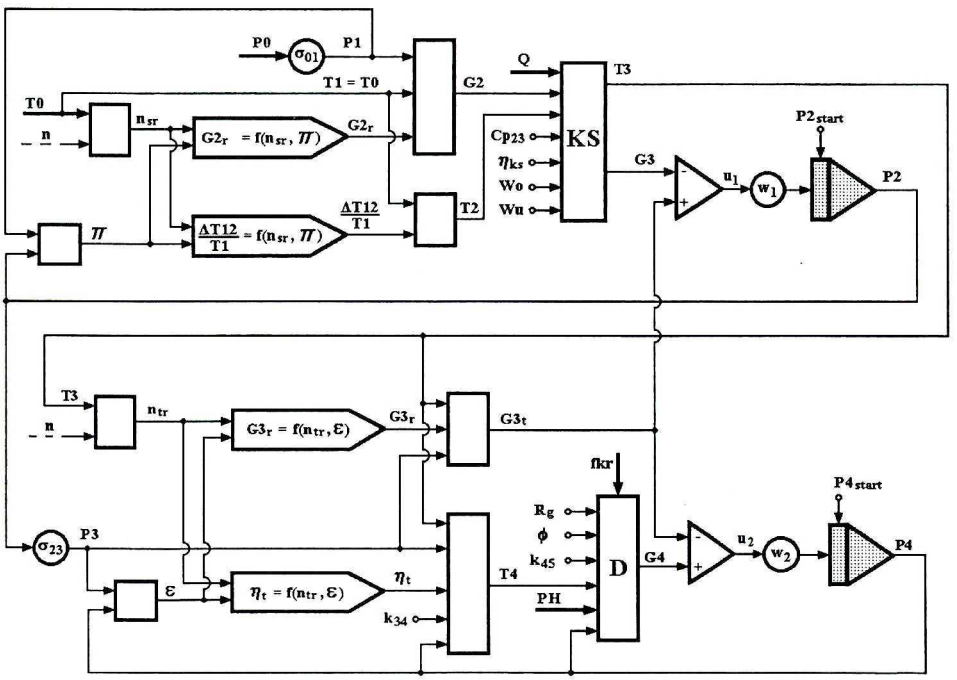

Fig. 6. Model B. A block diagram of the system of iteration to find roots of a system of algebraic equations that describe parameters of the working-medium flow

The above-described operations are repeated until both errors of iteration (u_1, u_2) reach sufficiently low values. The convergence of iterations for the full range of the model's operation (in this case: for the range of rotational speed starting with idle run up to full thrust) has been ensured by means of suitable selection of values of w_1 and w_2 factors.

4. Simulation of the engine fuel-supply and control system

Experiments with simulation models of the SO-3 engine should be similar to corresponding experiments feasible with a real engine. Therefore, an idea arises to join a simulation model of an engine with a simulation model of a real engine's fuel-supply system and controls. The real engine's fuel-supply system and controls composes a very complicated set of hydromechanical as well as pneumatic-and-mechanical units. The block diagram shown in Fig. 7 describes – in a simplified way, yet sufficient for conducting and understanding simulation experiments discussed below – a principle of operation thereof.

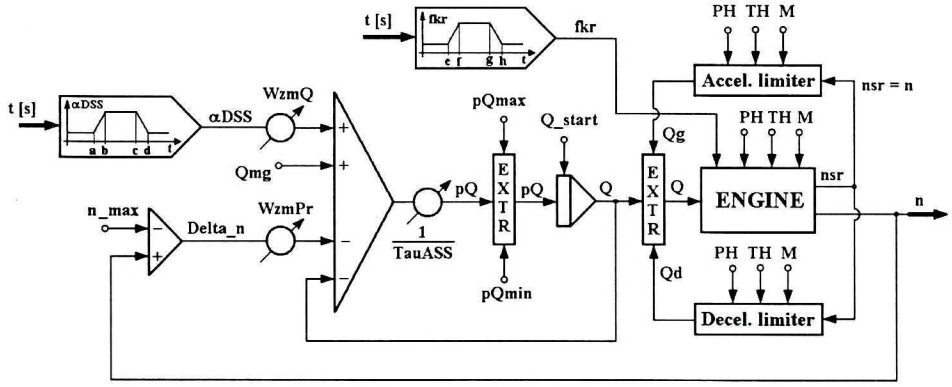

Fig. 7. A block diagram of the engine fuel-supply and control system

What can be found is that within the range of rotational speed from the idle run up to the value n ≤ n_max the open-loop control is executed, where some value of the steady-state rate of fuel flow (Q) is a function of the engine-control-lever angle (αDSS). In transient states, e.g. in the course of full acceleration, the actual value of the rate of fuel flow is bounded from above by means of the value limiter shown in the diagram (Qg). By analogy, in the course of deceleration limited is the actual minimum value of the rate of fuel flow (Qd). A proportional controller-limiter of the maximum rotational speed (n_max) also appears in the diagram.

Since simulation-based investigation has been limited to the engine's running under standard weather conditions on the ground (Ph = 760 mm Hg, Th = 288.2 K, M = 0), there is no barometric correction for the rate of fuel flow shown in Fig. 7. This correction, necessary in the case of changes in flight altitude and air speed, occurs in actual situation. That is why the in the diagram shown value of the reduced rotational speed (nsr) equals some physical value (n). Therefore, Qg = f(n,PH,TH,M), Qd = f(n,PH,TH,M). It also means that the limiters of actual values of the rate of fuel flow in the

course of acceleration (Qg) or deceleration (Qd) operate in a quasi-static way. Just as with an actual control system, it has been assumed that any change in the rate of fuel flow (Q) resulting from any shift of the engine control lever (αDSS) and possible actuation of the maximum-rotational-speed limiter, is delayed due to the presence of some value of time constant of the automatic engine-control unit (TauASS – shown in the diagram).

5. Methods of performing simulation-based experiments

All simulation-based experiments introduced in this paper refer to the engine run under ground-level conditions (Ph = 760 mm Hg, Th = 288.2 K, M = 0). Input functions of transient processes were effected by means of non-linear function generators: αDSS = f(t) and fkr = f(t) (see Fig. 7).
Two series of experiments were carried out:

- In the first series, by means of the function generator αDSS = f(t), quick and full-range accelerations/decelerations of the engine were accomplished for some specific value of the critical jet area of the nozzle (fkr).
- In the second series, by means of the function generator fkr = f(t), simulated were responses of the engine to changes in the critical jet area of the convergent nozzle, for some specific rates of fuel flow (Q), separately for the idle-run range and the maximum-rotational-speed range. The specific values of the rates of fuel flow were reached by means of fixing the engine control lever (αDSS) in two suitable, constant positions.

Time- and phase-dependent simulated processes resulting from Model A and those from Model B have been plotted on common diagrams to facilitate comparisons between the results.

6. Parameters of simulation

From the standpoint of the objective of this paper, the following are the most important parameters of the simulation model A: volume of the combustion chamber (V_{ks}) and that of the nozzle (V_d). The volume of the combustion chamber of an actual engine SO-3, defined as the volume of the engine duct between the compressor outlet and the turbine inlet, is approx. 0.070 m^3, whereas the nozzle volume understood as that of the engine duct between the turbine outlet and the duct-outlet cross-section is approx. 0.05 m^3. The above defined values as applied to Model A make the obtained results differ only slightly from similar simulation-based results gained from Model B. This slight difference makes, in turn, that some significant scale-up of diagrams/plots is required to compare between these results. That is

why $V_d = 0.1$ m^3 has been assumed the least hypothetical value of the nozzle volume. In the series of experiments with Model A, simulated were processes for different values of convergent nozzle volume ranging from $V_d = 0.1$ to $V_d = 0.6$ m^3, each 0.1 m^3. For each simulation performed on Model A, the combustion-chamber volume $V_{ks} = 0.075$ m^3 was assumed. For both the models, the method of numerical constant-step rectangular integration was used.

7. Simulated full-range accelerations and decelerations

The most important results of full-range acceleration/deceleration simulations with Models A and B engaged are presented in Figs 8 and 9. Fig. 8 shows a series of 6 simulated time functions of rotor rotational speed (n) gained from Model A and superimposed on the plot of a similar function gained from Model B. To better show differences in results gained, the selected (and indicated in Fig. 8) portions of the plot have been scaled up and presented in Figs 8a and 8b.

What has been phase-mapped in Fig. 9, are 6 time functions of actual average impact temperature of gas in the nozzle (T4) against engine rotational speed (n), gained from Model A and superimposed on those gained from Model B. Figs 9a and 9b show scaled-up portions of Fig. 9.

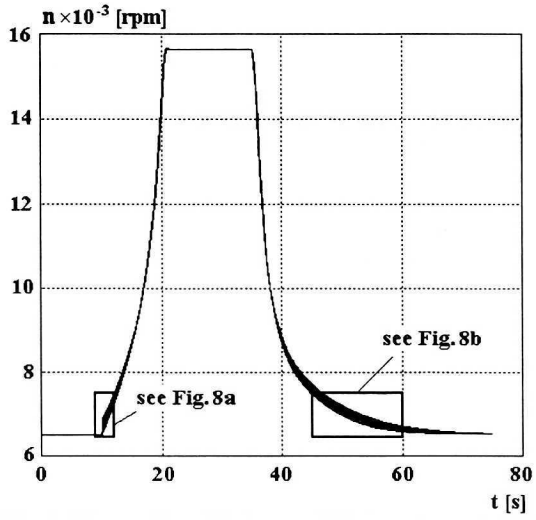

Fig. 8. Comparison between rotational-speed plots gained from Model A and Model B

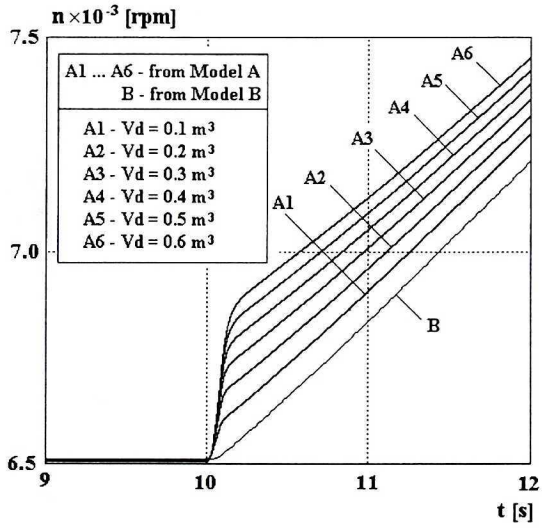

Fig. 8a. Comparison between rotational-speed plots gained from Model A and Model B

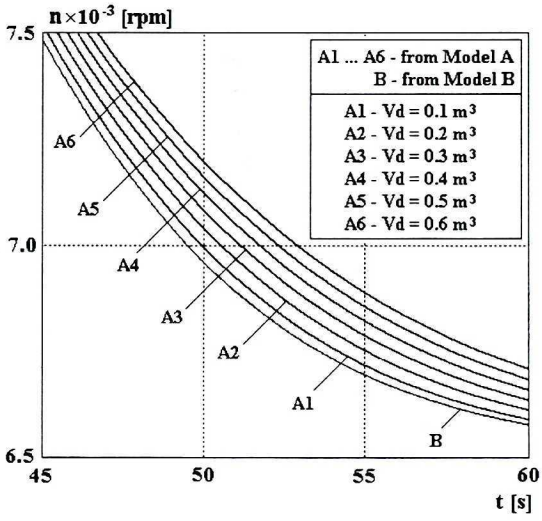

Fig. 8b. Comparison between rotational-speed plots gained from Model A and Model B – a portion of the plot selected from Fig. 8

The simulated time functions of average impact temperature of gas in the nozzle (T4), shown in Fig. 9, considerably differ from those recorded in the course of tests with an actual SO-3 engine. Responsible for these discrepancies are dynamic errors (difficult to compensate for) of measurements, i.e. of actual values of temperature, taken on an engine by means of a set of thermocouples. More detailed discussion on this issue of great significance exceeds the limits of this paper [10].

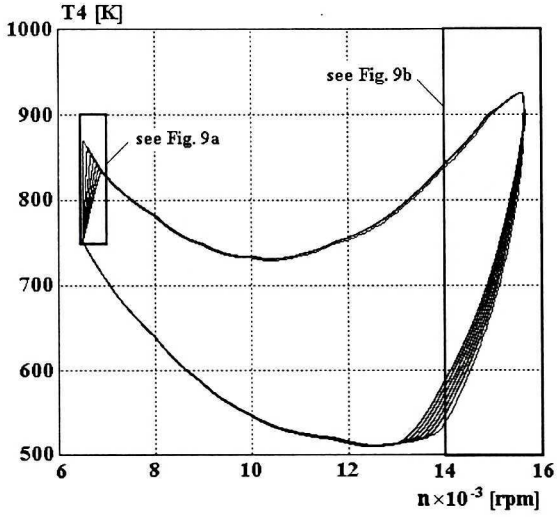

Fig. 9. Gas temperature in the nozzle against rotational speed – comparison between results gained from Models A and B

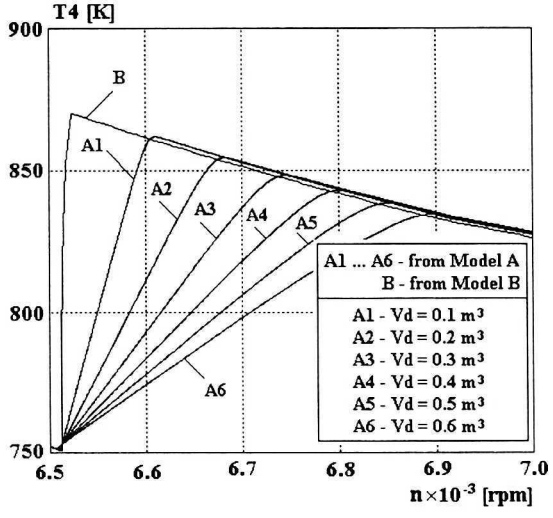

Fig. 9a. Gas temperature in the nozzle against rotational speed – comparison between results gained from Models A and B – a selected portion of the plot(s) in Fig. 9

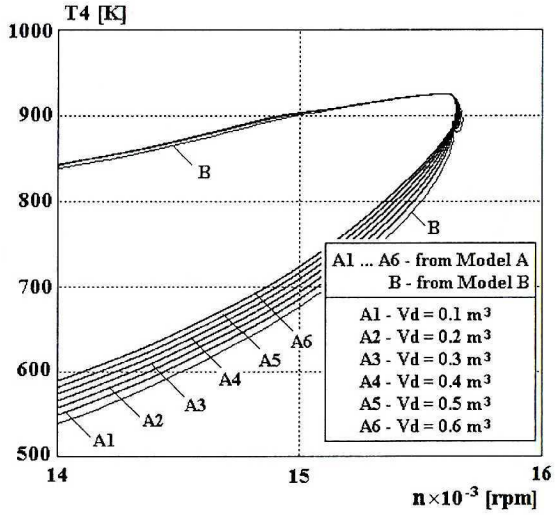

Fig. 9b. Gas temperature in the nozzle against rotational speed – comparison between results gained from Models A and B – a selected portion of the plot(s) in Fig. 9

8. Simulated responses to changes in the jet area of the nozzle

Simulated responses of engine parameters to changes in the jet area of the convergent nozzle (fkr) were investigated for some specific positioning of the engine control lever, i.e. in the idle-run position (αDSS = 0 deg), and steady-state conditions of engine running (n = n_bj). They are presented as time functions in Fig. 10.

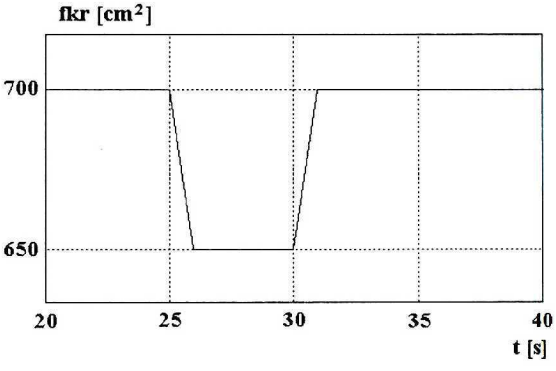

Fig. 10. Time function due to a change in the jet area of the nozzle

Three simulated time functions of the rotor rotational speed (n) gained from Model A and then superimposed on the plot of a similar function gained from Model B are shown in Fig. 11. This time, unlike with results presented

in Figs 9 and 10 and to make the plots legible, only three (3) curves from Model A have been shown for the following cases: V_d = 0.2, 0.4, 0.6m^3. A similar procedure was applied in the case of simulation-effected functions of average impact temperature of gas in the nozzle (T4).

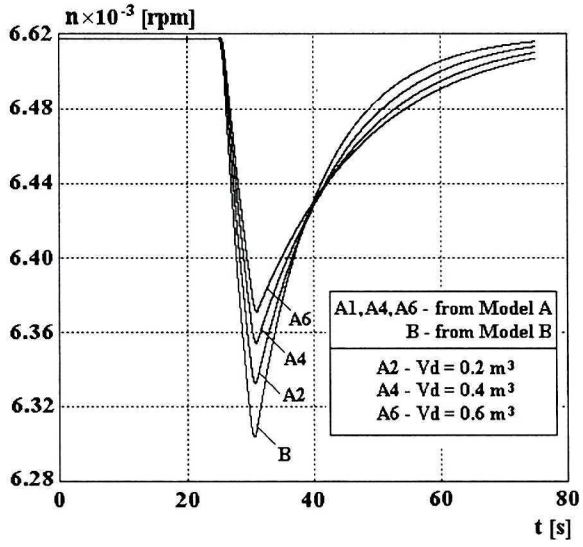

Fig. 11. Rotational speed versus time – comparison between results gained from Models A and B

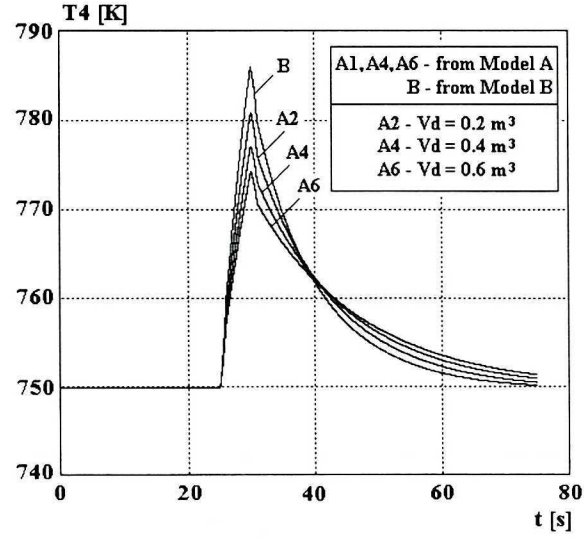

Fig. 12. Time functions of gas temperature in the nozzle – comparison between results gained from Models A and B

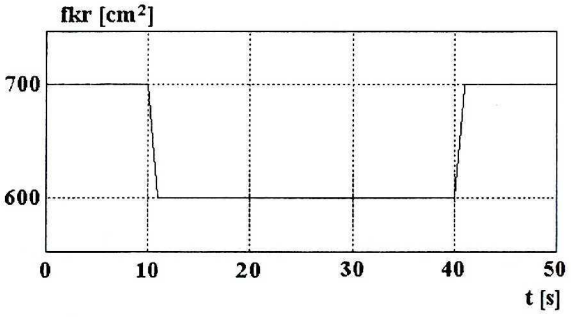

Fig. 13. Time function due to a change in the jet area of the nozzle

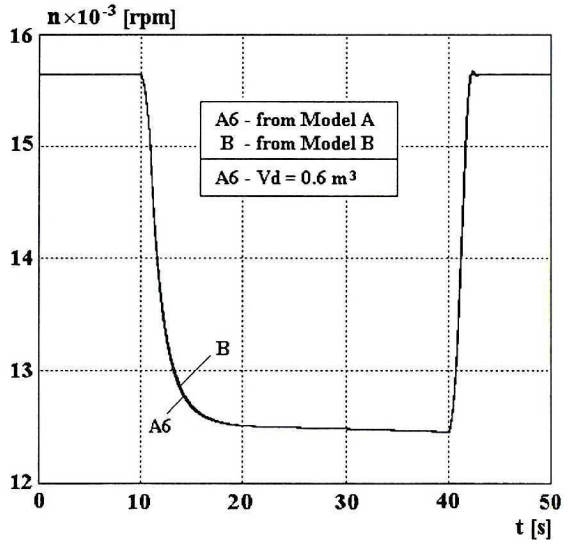

Fig. 14. Comparison between rotational-speed functions gained from Models A and B

Figures 14 and 15 illustrate effects of rotational-speed (n) response and impact temperature of gas (T4) on changes in critical jet area of the convergent nozzle (fkr) in the course of engine's steady-state operation within the maximum range of rotational speed (n = n_max). This time accomplished was the excitation in the form shown in Fig. 13. In this case as well, to make the plots legible, only one simulated time function gained from Model A has been shown for the nozzle volume $V_d = 0.6$ m^3. Then, it was superimposed on that gained from Model B. Figs 15a and 15b show scaled-up portions of Fig. 15.

The simulated time functions of average impact temperature of gas in the nozzle (T4), shown in Fig. 15, differ considerably from those recorded in the course of testing an actual SO-3 engine. Responsible for these discrepancies are the above-mentioned dynamic errors (related to plots shown in Fig. 9)

of measurements, i.e. of actual values of temperature, taken on an engine by means of a set of thermocouples.

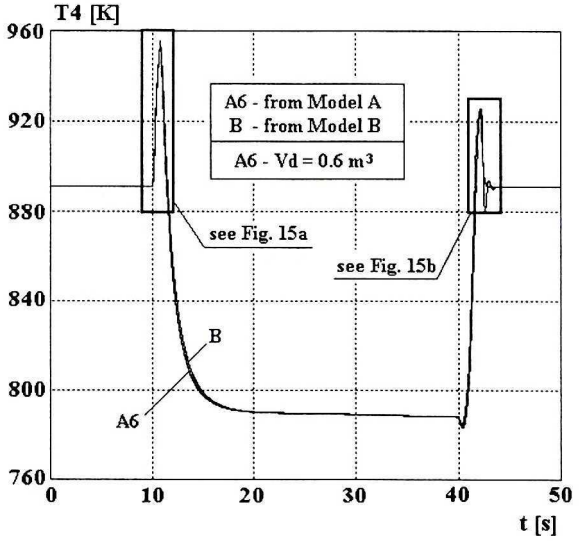

Fig. 15. Time functions of rotational speed – comparison between results gained from Models A and B

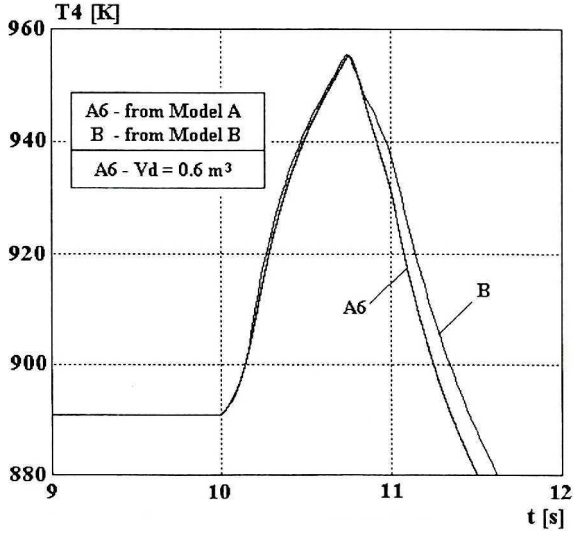

Fig. 15a. Temperature of gas in the nozzle against rotational speed.
Comparison between results gained from Models A and B – a portion selected from Fig. 15

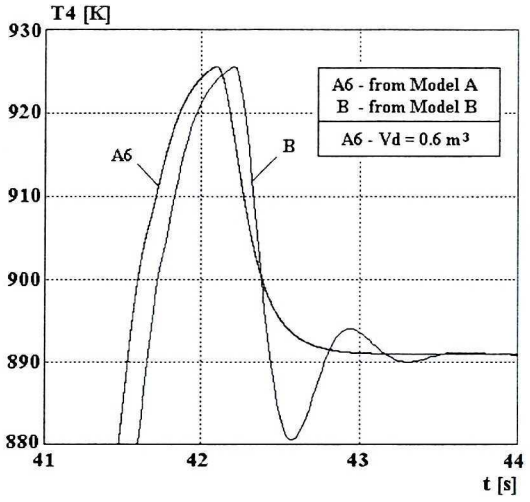

Fig. 15b. Temperature of gas in the nozzle against rotational speed.
Comparison between results gained from Models A and B – a portion selected from Fig. 15

9. Conclusions

Differences between simulation-effected results gained from Model B and those from Model A, for the lowest nozzle capacity taken into account (V_d = 0.1 m^3), are negligibly small from the standpoint of the modelling objective. In particular, they are scarcely noticeable for the range of higher rotational speeds. For the range of low rotational speeds, the differences are observable, however, lower than errors of the simulation method itself. These errors are caused by a number of factors, which give grounds for the mathematical modelling of an engine. These factors might be as follows: acceptance of a one-dimensional description of flow of the working medium, inaccuracy of applied static characteristics of the turbine and the compressor, a simplified way of describing – in a mathematical way – the combustion chamber, acceptance of constant values of specific heat and isentropic exponents of the working medium.

The following specific properties of aircraft turbine engines can prove significant limits to the accuracy of modelling:

- Well-marked differences between performance-related characteristics of different engines of the same type, resulting from the usual production-effected dispersion.
- Easy to observe – throughout suitably long time intervals – degradation in performance of specific engines due to usual wear and tear [13].
- The dynamics of the rotor acceleration and deceleration cannot be precisely described due to considerable effects of thermal deformations (observed in the course of the operational use) of the engine duct and in

particular, of the engine turbine, nozzle, and labyrinth seals [5]; also, of deformations of gas-temperature distributions at the combustion-chamber outlet [2], [6], [8].

Therefore, any attempt to perform very accurate modelling proves unjustified. To recapitulate, the method applied to generate Model B proves suitable to formulate a simulation-based model of the SO-3 engine treated as a controlled source of thrust to provide propulsion to an aircraft. On the other hand, the method applied to generate Model A proves well grounded with engines furnished with nozzles mounted at the end of suitably long (tail) exhaust pipes. Typical are engines furnished with afterburners.

A simplified method of engine modelling, with the dynamics of the processes of accumulation of the working medium's mass and enthalpy disregarded, can also be used to develop relatively simple algorithms of the so-called non-linear observers [11], [12]. The observers are of potentially great practical importance, in particular, to monitor non-measurable or difficult to measure parameters of operation of turbine jet engines. These may include actual values of thrust, temperature at the combustion-chamber inlet, mass flow of the working medium, etc.

The Author supposes that the above-formulated conclusions could prove reliable in the case of turbine engines featured with similar values of both maximum pressure ratios (π) and maximum mass flows of the working medium (G4), as with the SO-3 engine. This is what results from the careful examination of simulation effects. On the above-presented plots one can find that the greatest effect of the nozzle volume (V_d) is observed for the range of low rotational speeds (n) of the engine where, at the same time, the pressure ratio and the mass flow of the working medium are low (Figs 8, 9). For the range of high rotational speeds, featured with high pressure ratio and high mass flow of the working medium, the influence of the nozzle volume is dramatically reduced to the level, at which making it noticeable requires considerable reduction of the number of occurrences of this parameter down to three in Figs 11 and 12, and to only one in Figs 14 and 15, which is the greatest out of six occurrences assumed.

Table 1.

Comparison between times of simulation with Model A and B engaged (Figs 14, 15)

Model	Integration step [ms]	Duration of actual proces [ms]	Duration of simulation [s]
Model A	0.2	50	126
Model B	20	50	6

From the foregoing it clearly follows that there is a great need for similar simulation-based experiments with turbine engines of much higher ranges of

the pressure ratio and the mass flow of the working medium, i.e. for engines like RD-33 or F100-PW-229. The Author supposes that, on the grounds of comparing simulation-effected results for a wider range of turbine engines, it would be possible to formulate some objective numerical criterion. It will be used to decide if in the simulation-based model there is a need – in some specific cases – to take account of the dynamics of the process of accumulating mass and enthalpy of the working medium. It is of great importance because of much greater rate of performing digital simulation on Model B than on Model A. To compare both instances, Tab.1 shows measurements of duration of simulation of the same process accomplished with each of the models. The simulation was performed by means of a digital computer. Times shown were gained on the microcomputer PC furnished with the Pentium processor (R), the 3.0 GHz CPU-clock and 1.0 GB RAM. Codes of numerical procedures of both the models were not subject to optimisation aimed at the minimisation of time of computer accomplishment thereof.

It was mainly the need to apply a very short integration step, well matched to the fastest process performed in the model, that made time of simulation with Model A considerably longer. The fastest process mentioned is the process of accumulating mass and energy in the least selected duct volume, i.e. in the combustion-chamber volume (V_{ks}). In Model B, the integration step has to be well matched to the slowest dynamic process in the engine, i.e. to the process of accumulating kinetic energy in the rotor mass. For this reason, it may prove many times longer than the integration step in Model A.

Manuscript received by Editorial Board, April 03, 2006;
final version, December 28, 2006.

REFERENCES

[1] Dobrianskij G. W., Martianova T. S.: Dinamika Aviacjonnych GTD. Mašinostrojenije, Moskwa 1989.

[2] Identyfikacja wpływu stanu technicznego turbinowych silników odrzutowych na rozkład pola temperatury przed turbiną. Projekt badawczy KBN Nr 8T12D01421. Data ukończenia: lipiec 2003.

[3] Korczewski Z.: Modelling Gas-Dynamical Processes within a Turbocharging System of a Marine Four-Stroke Engine. Journal of KONES Internal Combustion Engines. Warsaw – Gdynia 2001.

[4] Olifirof F. N., Martynof W. N., Michajlof A. A., Dolgolenko G. P., Wiernyj L. I., Dmitriev W. G., Dolženkov N. N.: Integrirovannaja Sistema Ypravlenija Silovoj Ustanovki SWWP. Wiestnik MAI, t. 3, Nr 1, 1996.

[5] Osiński J., Pawlak W., Szot A.: Deformacja i naprężenia termiczne zewnętrznej powłoki dyszy turbinowego silnika odrzutowego. Biuletyn Wojskowej Akademii Technicznej. Vol. LIII, Nr 1(617), Warszawa, 2004.

[6] Pawlak W. I., Balicki W.: Influence of an Unequality of Gas Thermal Field at the Jet Engine Turbine Inlet on to the Speed of Transient Processes – the results of experiments with real engine. Journal of KONES Internal Combustion Engines, Vol. 10, Warsaw 2003.
[7] Pawlak W. I., Wiklik K., Morawski J. M.: Synteza i Badanie Układów Sterowania Lotniczych Silników Turbinowych Metodami Symulacji Komputerowej. Biblioteka Naukowa Instytutu Lotnictwa, Warszawa 1996.
[8] Pawlak W. I.: Influence of an Unequality of Gas Thermal Field at the Jet Engine Turbine Inlet on to the Speed of Transient Processes – Result of Experiments with simulation Model. Journal of KONES Internal Combustion Engines, Vol. 7, Warsaw – Lublin, 2000.
[9] Pawlak W. I.: Monitorowanie osiągów silników K-15 na samolocie I-22 IRYDA. Polskie Towarzystwo Mechaniki Teoretycznej i Stosowanej, Mechanika w Lotnictwie „ML-VIII" Warszawa 1998.
[10] Pawlak W. I.: Problemy monitorowania niskocyklowych obciążeń termicznych lotniczego silnika turbinowego. V Krajowa Konferencja „Diagnostyka Techniczna Urządzeń i Systemów DIAG'2003", Ustroń, 13–17 paźdź. 2003.
[11] Pawlak W. I.: Zastosowania Nieliniowych Obserwatorów Parametrów Pracy Turbinowego Silnika Odrzutowego. 27th International Science Conference on Combustion Engines KONES 2001, September 9–12, 2001, Jastrzębia Góra, Poland. Conference Proceedings.
[12] Pawlak W. I.: Non-Linear Observer of single-Rotor Single-Flow Jet Turbine Engine during Operation. Journal of KONES Internal combustion Engines. Vol.12, No 1–2, Warsaw 2005.
[13] Pomiar widma cyklicznych obciążeń jednowirnikowego jednoprzepływowego turbinowego silnika odrzutowego w eksploatacji wspomagany komputerową symulacja parametrów jego pracy w stanach nieustalonych. Projekt badawczy KBN Nr 9T12D00717. Data ukończenia: czerwiec 2001.
[14] van Essen H. A., de Lange H. C.: Nonlinear Model Predictive Control Experiments on a Laboratory Gas Turbine Installation. Transactions of the ASME, Journal of Engineering for Gas Turbines and Power, April 2001, Vol. 123.

Wpływ objętości dyszy zbieżnej na procesy przejściowe turbinowego silnika odrzutowego

Streszczenie

W naukowych publikacjach na temat matematycznego modelowania silników turbinowych (traktowanych jako obiekty sterowania i automatycznej regulacji), często mówi się o wpływie procesów akumulacji masy i entalpii czynnika roboczego na dynamikę ich procesów przejściowych. W niniejszej pracy przedstawiono porównanie wyników symulacji przeprowadzonej na dwóch wariantach modelu turbinowego silnika odrzutowego typu SO-3. W pierwszym wariancie uwzględniono dynamikę procesów akumulacji masy i energii czynnika roboczego w objętości komory spalania oraz w objętości dyszy zbieżnej. W drugim, uproszczonym wariancie modelu, zaniedbano dynamikę akumulacji masy i energii czynnika roboczego, zakładając, że w obrazie procesów przejściowych dominuje dynamika akumulacji energii kinetycznej przez masę wirnika. W celu przeprowadzenia eksperymentów symulacyjnych obie wersje modelu silnika łączono ze specjalnym blokiem symulacyjnym, imitującym działanie układu zasilania i sterowania. Wykonano dwie serie eksperymentów. W pierwszej obserwowano przebiegi procesów przejściowych wywołane szybkim przestawianiem dźwigni sterowania z pozycji biegu jałowego do pozycji pełnego ciągu – i z powrotem. W drugiej serii obserwowano procesy wywołane tylko zmianami pola powierzchni przekroju krytycznego dyszy. Na drugim wariancie modelu zbadano wpływ coraz większych, hipotetycznych objętości dyszy, na przebiegi procesów przejściowych. Stwierdzono, że w przypadku silnika SO-3 mała objętość dyszy ma niewielki wpływ na przebieg procesów przejściowych, zatem uproszczona metodyka jego modelowania jest uzasadniona.